Individual Cylinder Air-Fuel Ratio Control with a Single EGO Sensor

Jessy W. Grizzle, *Senior Member, IEEE,* Kelvin L. Dobbins, and Jeffrey A. Cook, *Associate Member, IEEE*

Abstract—**An approach to achieving uniform cylinder-to-cylinder air-fuel ratio control in the face of injector mismatch and unbalanced airflow due to engine geometry is presented. A key feature of the proposed method is that it functions well with the switching-type exhaust gas oxygen sensor commonly used in today's automobiles. The controller design from modeling to experimental implementation in a dynamometer test facility is documented.**

I. Introduction

A. Background and Motivation

THE electronic fuel control system of a modern spark ignition automobile engine employs individual fuel injectors located in the inlet manifold runners close to the intake valves to deliver precisely timed and accurately metered fuel to all cylinders. This fuel management system acts in concert with the three-way catalytic converter (TWC) to control HC, CO, and NOx emissions. Fig. 1 illustrates the conversion efficiencies provided by a typical TWC as a function of exhaust air-fuel ratio (A/F) for the three constituents [1]. It can be seen that there is only a very narrow range of A/F near the stoichiometric value (14.64) over which high simultaneous conversion efficiencies may be attained. In order to use the TWC effectively, feedback from an exhaust gas oxygen (EGO) sensor in the vehicle exhaust system is utilized to regulate the A/F operating point. A block diagram of this system is illustrated in Fig. 2, [1]. The EGO sensor used in this system incorporates a ZrO_2 ceramic thimble employing a platinum catalyst on the exterior surface to equilibrate the exhaust gas mixture. The interior surface of the sensor is exposed to atmosphere. Because output voltage is exponentially related to the ratio of O_2 partial pressures across the ceramic, the sensor is essentially a switching device indicating by its state (practically, 0 or 1 V) whether the exhaust gas is rich or lean of stoichiometry. The sensor response time to a step change in A/F is typically less than 300 ms [4]. As shown in the block diagram of Fig. 2, this signal is fed back through a comparitor and digital PI controller to adjust the fuel injector pulsewidths so as to achieve an average A/F close to stoichiometry, and therefore within the high efficiency "window" of the TWC.

It should be noted that although the average A/F is controlled to perceived stoichiometry, individual cylinders may be operating consistantly rich or lean of the desired value. This cylinder-to-cylinder A/F maldistribution is due in part to injector variability. Consequently fuel injectors are machined to close tolerances to avoid individual cylinder flow discrepancies, resulting in high cost per injector. However, even if the injectors are perfectly matched, maldistribution can arise from individual cylinders having different breathing characteristics due to a combination of factors such as intake manifold configuration and valve characteristics. Shulman and Hamburg [1] have shown that such cylinder-to-cylinder A/F maldistribution can result in increased emissions due to shifts in the closed loop A/F setpoint relative to the TWC. Similar effects are presented in Colvin *et al.* [3].

This paper describes the development of a controller for tuning the A/F in each cylinder of a four cylinder engine to eliminate maldistribution; six or eight cylinder engines could be treated in a similar manner. Section II develops a mathematical model of the A/F loop in a modern fuel-injected engine. In

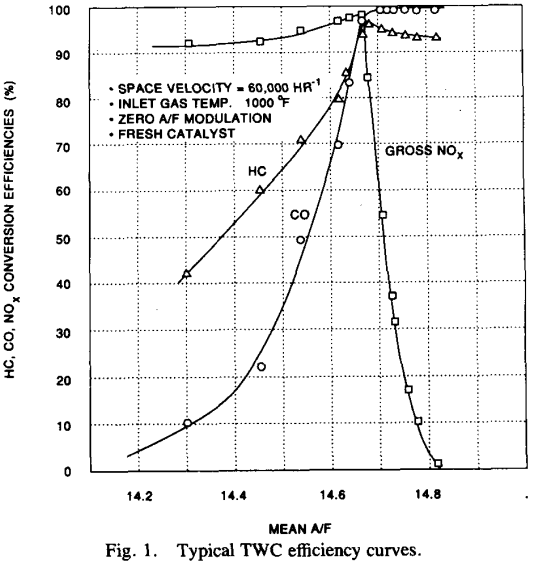

Fig. 1. Typical TWC efficiency curves.

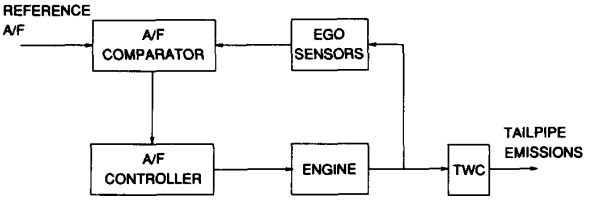

Fig. 2. Ubiquitous A/F feedback loop employing exhaust gas oxygen sensor.

Manuscript received December 1989; revised August 1990. This work was supported in part through matching funds provided by the Ford Motor Company to Grant NSF ECS-88-96136.

J. W. Grizzle is with the Department of Electrical Engineering and Computer Science, University of Michigan, Ann Arbor, MI 48109-2122.

K. L. Dobbins and J. A. Cook are with the Ford Motor Company Scientific Research Laboratory, P.O. Box 2053, SRL Room S2093, Dearborn, MI 48121-2053.

IEEE Log Number 9041743.

0018-9545/91/0200-0280$01.00

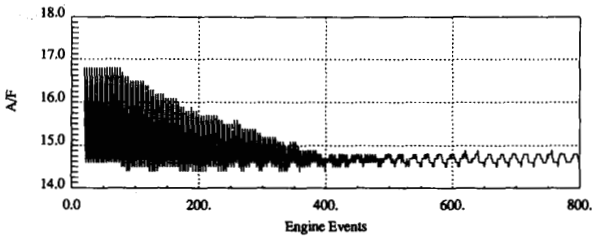

Fig. 3. Simulated A/F trace of controller eliminating maldistribution.

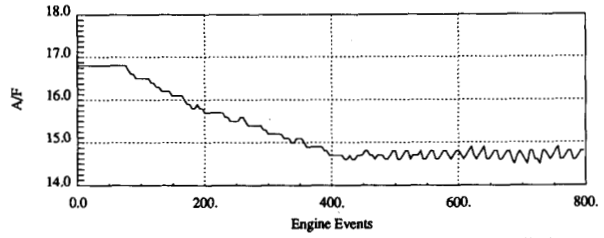

Fig. 4. Simulated trace of A/F in cylinder 2 while controller eliminates maldistribution.

Section III, details of the design of the controller are presented; its main feature is that it uses only the information provided by the single existing EGO sensor. The controller was implemented in an engine dynamometer facility. The experimental set-up and the test results are described in Section IV, along with a method for achieving an extended operating region based upon scheduling the sampling.

The next subsection provides a preview of the controller's operation.

B. What the Controller Does

In order to have an idea of how the controller performs, consider Fig. 3. It shows the results of a simulation model of the air-fuel loop when the fuel injectors are imbalanced: cylinder 2 is 20% lean, while the remaining cylinders are nominal. For the first 70 engine events, only the existing onboard control strategy is being employed. Note the greatly varying A/F at the EGO sensor, which could adversely affect the catalyst efficiency and life time. It is worth noting that no existing sensor or laboratory instrument is fast enough to register the full extent of the A/F excursion, and this shows one of the advantages of a good mathematical model: it allows you access to difficult to measure quantities. At 70 engine events, the individual cylinder A/F controller is enabled, and in about 350 engine events completely eliminates the A/F maldistribution and returns the system to its classical limit cycle behavior. Fig. 4 shows once again a simulated signal from the model, under the same conditions as above, but this time a signal that is easily measurable: namely the A/F in the exhaust runner of cylinder 2 (it can be experimentally measured by placing a linear-type EGO in the corresponding runner of the exhaust manifold;[1] such a signal is not available for control purposes). The efficacy of the individual cylinder A/F controller in eliminating the A/F maldistribution is evident. In Section IV, collaborating *experimental data* collected in an engine dynamometer are reported; the reader should compare Fig. 8(d) with Fig. 4.

[1]Such sensors typically have a much lower bandwidth than the switching-type sensor, but since the A/F in a given runner is not rapidly varying, this is not an issue.

II. System Model

The fuel system used on the four cylinder engine on which the controller has been implemented requires two major operations: air flow sensing and fuel injection timing. Air flow measurement is accomplished by a volume flow meter, the output signal of which is corrected for barometric pressure to provide mass rate information. Fuel injection timing is sequential, such that each injector event coincides with the beginning of the intake stroke of the associated cylinder. A block diagram of the A/F control loop for this engine is depicted in Fig. 5. The input to the system model is the mass air flow signal. The model contains representations of the individual fuel injectors, cylinders and exhaust manifold runners, the exhaust gas oxygen sensor, and the onboard microprocessor-based controller. The sampling rate $1/T$ indicated in the block diagram corresponds to the rate of occurrence of induction events;[2] that is for a four cylinder engine, T is the time required for the crankshaft to advance 180°, which, at 1500 r/min, for example, is 20 ms. In general, for engines of any cylinder configuration, the sample rate is related to the occurrence of induction events by the relationship $T = 120/nN$ s, where n is the number of cylinders and N is the engine speed in revolutions/minute.

The intake manifold has been modeled as a first-order lag since it is essentially a capacitive volume with flow resistance. The air meter is assumed to be ideal, with the estimated air charge of a cylinder being given by the integral of the mass flow rate of air over one engine event, (that is, 180 crankangle degrees or T units of time). The fuel injectors are represented by the unknown gains $G(1)$–$G(4)$. The four events that an air-fuel charge spends in a cylinder, plus the time it takes to travel the length of an exhaust manifold runner, is lumped together in the pure delay terms $\exp(-d_i s)$. The terms $1/(\tau_i s + 1)$ are to account for mixing between the air-fuel charges associated with a single cylinder. The blocks $\exp(-d_e s)$ and $1/(\tau_e s + 1)$ account for any additional transport delay and mixing incurred between the confluence of the exhaust runners and the EGO sensor. The latter is modeled as a first-order lag followed by a preload (i.e., relay or switching-type) nonlinearity. Finally, the existing onboard controller is assumed to be proportional plus integral.

The system model depicted in Fig. 5 has proven useful for analyzing the effects of disturbances on the A/F loop, for investigating the effects of changing the sample rate of the digital controller, and for determining the deleterious effects of cylinder-to-cylinder maldistribution. Note that maldistribution arising from inequities in the air flow among different cylinders has not been specifically taken into account. However, as we are only concerned with the ratio of air to fuel, this is without loss of generality since it can be lumped into the injector gains.

For the purpose of designing a controller to individually adjust the fuel injectors, we will make several (additional) simplifying assumptions. Firstly, it is supposed that the mass flow rate of air is constant. Secondly, the exhaust gas mixing in the individual runners, as well as between the runners and the sensor, can be neglected. Finally, the transport delays of the four exhaust runners are approximately equal. With these three assumptions, one arrives at the model of Fig. 6. Note that K is the sum of the transport delay in an exhaust runner and the delay between the runners and the sensor. The additional input v represents the trimming signal that is to be added for balancing the A/F among

[2]One can think of the four induction events in a four cylinder engine, or the events: induction, compression, combustion and exhaust.

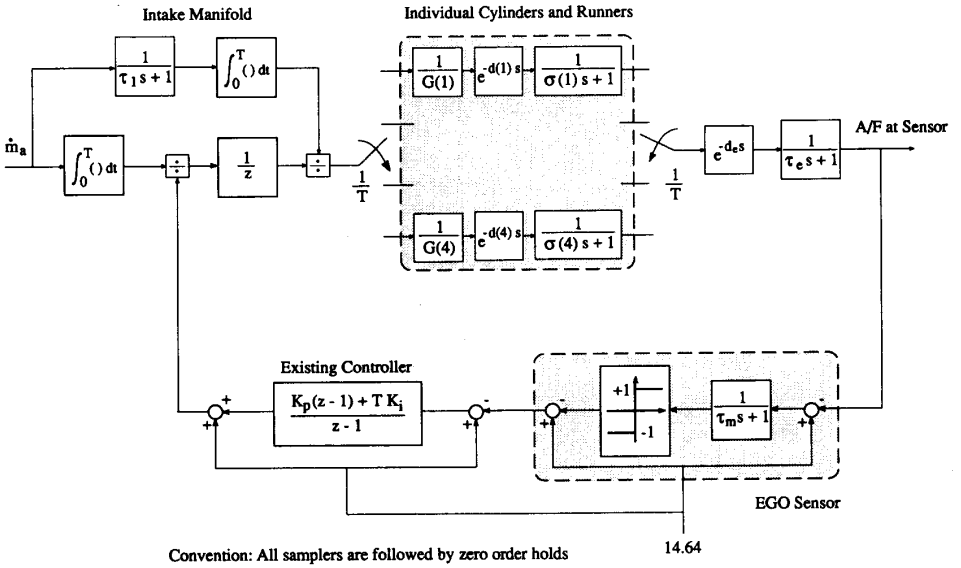

Fig. 5. Detailed A/F control loop.

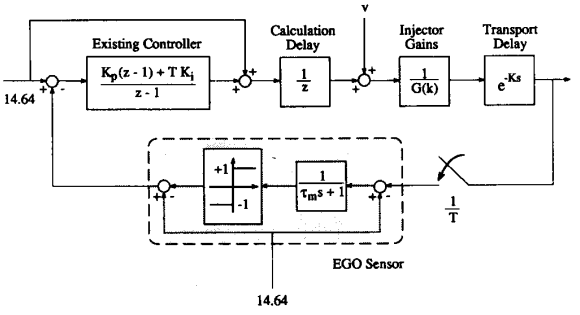

Fig. 6. Simplified A/F control loop.

the cylinders. In the actual implementation, it will be scaled to be a multiplication factor for the pulsewidth sent to an individual injector rather than the additive correction shown in the figure.

For definiteness and later use, nominal values for the parameters of the simplified model will be taken as: $K_P = 0.09$, $K_I = 0.33$, K = seven events, and $\tau_m = 0.07$ [4]. In the next section, we detail the design of a controller for asymptotically balancing the A/F in each of the cylinders.

III. Controller Design

The control objective is to maintain the A/F as close as possible to stoichiometry. The existing controller performs well when the cylinders are balanced, but its performance degrades significantly in the presence of maldistribution. We will show how the multirate sampling/periodic control techniques of [5]–[9] can be used to develop a controller which individually adjusts the fuel injectors and uses only the existing EGO sensor.

We start with the system model depicted in Fig. 6, with the nominal parameter values of the previous section, and replace the transport delay and the first-order lag in the EGO sensor with their discrete equivalents; that is, $1/z^7$ and $0.25/(z - 0.75)$, respectively. In addition, the preload nonlinearity in the EGO sensor is viewed as a (very) coarse form of quantization and is neglected in the initial design phase. This yields a linear time-varying, but 4-periodic model, (due to the periodically varying injector gains, $G(k) = G(k + 4)$, $k = 1, 2, \cdots$) of the general form

$$x_{k+1} = A(k)x_k + B(k)v_k + E(k)14.64$$
$$y_k = C(k)x_k, \tag{1}$$

where $v_k = v(kT)$ is the value of the trimming control and $y_k = y(kT)$ is the output of the EGO sensor, both at the kth engine event. By convention, top-dead-center of the exhaust stroke of cylinder 1 is the initial event, that is, t_0.

It is clear why a scalar constant coefficient PI controller cannot maintain the stoichiometric set point of 14.64 in each of the cylinders: the system with unbalanced cylinders is time-varying. What is needed, essentially, is an integral-type controller for each cylinder. Our goal is to accomplish this without placing additional sensors on the engine, and in particular, without putting a sensor in each of the exhaust runners.

The main step toward achieving this is to apply the "lifting technique" of [5], [7], [8] to obtain a time-invariant representation of the system. The essential idea is that if one block processes the inputs and outputs over intervals of time corresponding to the period of the model, which in our case is one complete engine cycle, the resulting model description is time-invariant, due to the very definition of periodicity: everything exactly repeats itself from one engine cycle to the next.

To effect this, let

$$V_j = \begin{bmatrix} v_{4j+1} \\ v_{4j+2} \\ v_{4j+3} \\ v_{4j+4} \end{bmatrix} \quad \text{and} \quad Y_j = \begin{bmatrix} y_{4j+1} \\ y_{4j+2} \\ y_{4j+3} \\ y_{4j+4} \end{bmatrix}; \tag{2}$$

in other words, V_j and Y_j are the vectors of controls and measurements corresponding to the jth engine cycle, which is comprised of events $4j + 1, 4j + 2, 4j + 3, 4j + 4$. Defining $\bar{x}_j = x_{4j}$, it follows that $\bar{x}$ evolves according to

$$\bar{x}_{j+1} = \bar{A}\bar{x}_j + \bar{B}V_j + \bar{E}14.64$$
$$Y_j = \bar{C}\bar{x}_j + \bar{D}V_j + \bar{F}14.64 \tag{3}$$

where

$$\bar{A} = A(4)A(3)A(2)A(1)$$
$$\bar{B} = \left[A(4)A(3)A(2)B(1) : A(4)A(3)B(2) : A(4)B(3) : B(4)\right] \tag{4}$$
$$\bar{C} = \begin{bmatrix} C(1) \\ C(2)A(1) \\ C(3)A(2)A(1) \\ C(4)A(3)A(2)A(1) \end{bmatrix}$$
$$\bar{D} = \left[\begin{array}{c:c:c:c} 0 & 0 & 0 & 0 \\ C(2)B(1) & 0 & 0 & 0 \\ C(3)A(2)B(1) & C(3)B(2) & 0 & 0 \\ C(4)A(3)A(2)B(1) & C(4)A(3)B(2) & C(4)B(3) & 0 \end{array}\right]$$

and $\bar{E}$ and $\bar{F}$ have the same form as $\bar{B}$ and $\bar{D}$ with the matrix E replacing B. For our particular system, it is possible to show that $\bar{D}$ and $\bar{F}$ are both identically zero.

It is emphasized that no input-output information has been lost in passing from (1) to (3); the signals have simply been collected and processed in "blocks" instead of one-by-one. The advantage of this representation is that it is time-invariant, irrespective of the injector gains, so that standard state space tools may be applied. Also, there are now four inputs and four outputs, corresponding to the number of cylinders, indicating that a controller will need 4-integrators in order to achieve independent set-point control over the four cylinders.

At this point, there are three options in the controller design: 1) leave the existing controller in place, unchanged, and add integral action on three of the four cylinders[3] in the new controller; 2) leave the proportional control action of the existing controller, but remove the integrator and then place an integrator on each of the four cylinders; 3) remove the existing controller entirely and start from scratch. For the purposes of this paper, we will take the latter approach.

We then need a state variable description of the path from v to y. It is convenient to let x^1–x^7 be the states of the transport delay and x^8 be the output of the EGO sensor, without the preload nonlinearity. This yields

$$x^1_{k+1} = \frac{1}{G(k)} v_k$$
$$x^{i+1}_{k+1} = x^i_k, \qquad i = 1, \cdots, 6$$
$$x^8_{k+1} = 0.75x^8_k + 0.25x^7_k$$
$$y_k = x^8_k. \tag{5}$$

Recall, however, the injector gains are precisely the unknown quantities, and so they must be replaced with the nominal value of 1 for the purpose of designing the controller; this gives a time-invariant model for which the formulas for the lifted system (3) simplify.

The design of the controller can now be completed as follows: Augment the lifted system with integrators,[4]

$$V(z) = \left(\frac{1}{z-1} \cdot I\right) W(z), \tag{6}$$

where I is the 4×4 identity matrix and W is the vector of new inputs. Next, design a stabilizing controller $W(z) = C(z)Y(z)$ for the augmented lifted system. There are of course many ways of doing this. We used the LQG approach here since the required operations are readily performed on a Computer Aided Control Systems software package. In particular, the cost function was chosen as

$$J = \sum_{j=1}^{\infty} Y_j^T Y_j + 100 W_j^T W_j; \tag{7}$$

in principle, the heavier weighting on the controls is aimed at achieving a fairly slow loop, but, since the system consists mainly of delays, this has limited effect. The noise covariances for the Kalman filter were selected as

$$\Sigma_{xx} = I + 100\tilde{B}\tilde{B}^T, \tag{8}$$

where I is the 12×12 identity matrix and $\tilde{B}$ is the "B" matrix of the lifted system augmented with the four integrators, and

$$\Sigma_{yy} = \begin{bmatrix} 6 & 2 & 2 & 2 \\ 2 & 6 & 2 & 2 \\ 2 & 2 & 6 & 2 \\ 2 & 2 & 2 & 6 \end{bmatrix}. \tag{9}$$

These choices were motivated by the loop transfer recovery results of [10]; the particular form of Σ_{yy} was an attempt to reflect correlation in the output components of the lifted system.

Carrying out the above yields a controller having 12 states, plus the four integrators. Its full implementation would require about 500 floating point operations, which is unfeasible for the A/F control application. However, this does provide a benchmark against which to compare a more practical reduced order controller. Fortunately, in our case, the controller eigenvalues are all well within the unit circle, and a drastic model order reduction could be performed. Indeed, we were able to keep only the dc-gain. This gave a final controller

$$V_{j+1} = V_j + MY_j \tag{10}$$

where

$$M = \begin{bmatrix} 0.0769 & 0.0220 & 0.0050 & -0.0312 \\ -0.0342 & 0.0782 & 0.0226 & 0.0059 \\ 0.0034 & -0.0337 & 0.0785 & 0.0232 \\ 0.0203 & 0.0036 & -0.0335 & 0.0793 \end{bmatrix}. \tag{11}$$

It requires only 16 multiplications and 20 additions,[5] to be

[3]Adding four integrators while leaving in the integrator in the existing controller results in an unobservable system.

[4]Alternately, augment the lifted system by $\bar{q}_{j+1} = \bar{q}_j + Y_j - Y_{\text{desired}}$.

[5]In practice, the physical signal from the EGO sensor is scaled to $+1$ and -1; thus, the multiply operations are replaced with simple logic operations.

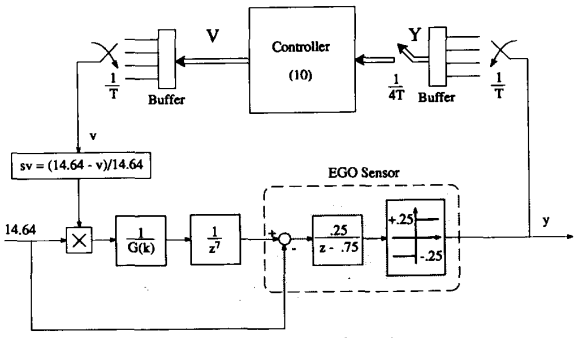

Fig. 7. Controller configuration.

performed once every engine cycle, that is, every four 180° increments of crankshaft revolution.

As mentioned earlier, in the actual implementation, the additive correction term (10) was converted into a scale factor for the pulsewidth used to drive the fuel injectors via

$$SV_j = (14.64 - V_j)/14.64; \tag{12}$$

this requires eight additional floating point operations.

The final system/controller configuration is shown in Fig. 7. The actual EGO sensor, with its nonlinearity, was incorporated by adjusting its "quantization" level to 0.25. This has the same effect as scaling the matrix M in the controller (10).

The effectiveness of the controller in eliminating maldistribution on the simplified model was already shown in Figs. 3 and 4; the next section discusses the implementation on an engine.

IV. Individual Cylinder Air-Fuel Ratio Control

A. Extended Controller Operation

The controller designed thus far is based on a linearized engine model at a single operating point. It is important to have a controller that operates over a wide range of engine speeds and loads. A conventional method of accomplishing this would be to design a multitude of controllers spanning the operating environment and schedule the application of these controllers with respect to speed and load (taking care that controller transitions are accomplished "seamlessly"). Fortunately, crankangle-based sampling combined with a serendipitous structure provides a model with an extended range of linear behavior [11]. Indeed, the only portion of the model which is a strong function of engine operating condition is the transport delay in the exhaust system. Consequently, one may expand the controller operating region while maintaining a constant controller structure by *scheduling the sampling* so that the total delay perceived by the controller is constant; that is, one accounts for increases or decreases in the transport delay through the addition of an offset to the sampling time, which is itself scheduled as a function of load and speed.

The basic idea is quite simple. Suppose the transport delay from the exhaust ports to the EGO sensor increases from seven engine events to 7 1/4 when the speed is reduced from 1500 to 1200 r/min. Then the time that the first sample in the kth data block Y_k is taken should be delayed by 45 crankangle degrees, and the subsequent samples taken at 180 crankangle degree intervals thereafter, just as before. Similar reasoning applies when the engine speed and/or load are increased, resulting in a decreased transport delay: the time that the first sample in a given block is taken must be advanced by a certain number of crankangle degrees. Creating a table of transport delay versus engine speed and load is straightforward. In the laboratory, the easiest method to implement this idea is to oversample the EGO sensor signal and keep multiple cycles of sensor data in a circular queue. Then the desired measurements can be picked out by shifting either forward or backward to account for an increased or decreased delay in the exhaust system.

B. Experimental Setup

The controller of the last section has been implemented in an engine dynamometer/real-time control systems laboratory [12]. This facility is equipped to measure, display, and record the inputs and outputs of the engine, actuators and sensors for parameter identification and model validation, and also to display and record controller and model outputs during the development and testing process. A novel feature of this facility is the ability to interface real hardware with a simulation model of the engine that has been implemented on a very high speed digital computer, an AD-10. The laboratory is fully linked with a corporate wide computer network, where the majority of the computer aided control engineering is performed.

The controller's implementation involved three processors. The existing 16-b microprocessor used on the production engine was kept to calculate the base pulsewidth for the fuel injectors. A patch was made in the production control strategy to disable its PI controller and to allow the insertion of the new control signals. A separate 16-b digital signal processing chip was used to synchronize the controller with intake and exhaust valve timing. The individual cylinder controller was implemented on a 32-b microprocessor, with the algorithm programmed in C. The microprocessors communicate with each other via dual port memory interfaces. A video display is used to monitor the operation of the controller. A switch was inserted to allow the operator to select between the existing controller and the proposed controller. All of this was done to allow us to do the development work in a user friendly environment.

The plant hardware consists of a port fuel injected four cylinder internal combustion engine together with its associated actuators and sensor. The exhaust manifold configuration is a 4 into 2 into 1 with the oxygen sensor located at the point where the pairs of exhaust runners converge. The output shaft of the engine is connected to an electric dynamometer, which allows the load to be controlled as a function of speed.

C. Test Results

Tests were performed on the engine dynamometer to verify the performance of the individual cylinder fuel controller over a wide range of operating points. The test data reported here were taken at 1500 r/min and 38 psi BMEP (brake mean effective pressure), and are typical of results obtained at other points. Individual cylinder A/F maldistribution was simulated by manually adjusting each of the injector pulsewidths about its balanced trim value. This balanced trim value was determined using EGO sensors located in each exhaust runner; once again, these signals are not available to the controller. The output of the conventional controller[6] (LAMBDA) and the outputs of the individual cylinder controller (SV_{1-4}) were recorded during the test. The output of the EGO sensor located at the confluence of the exhaust runners is measured and recorded along with the output of a linear type EGO sensor that was placed in the exhaust

[6]Commanded A/F divided by 14.64.

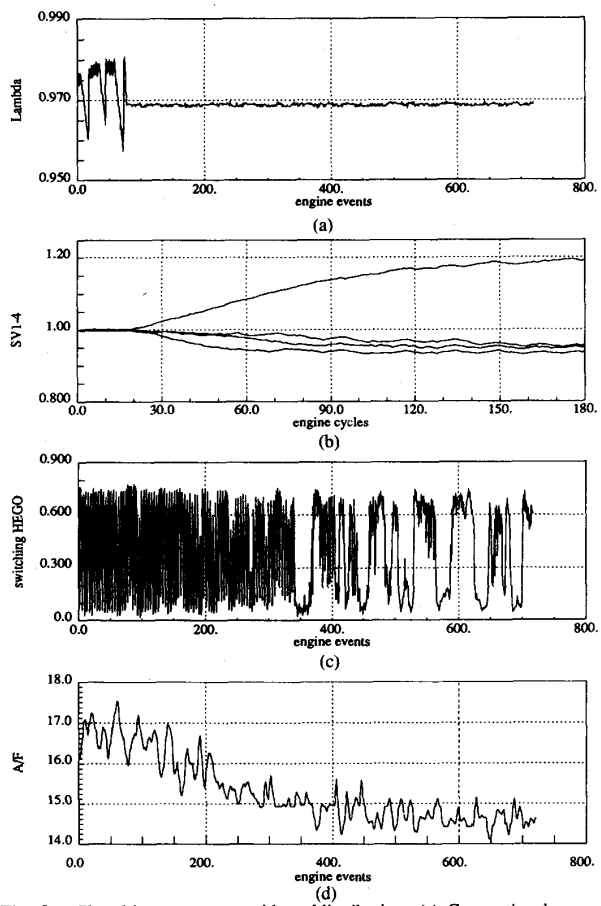

Fig. 8. Closed-loop response with maldistribution. (a) Conventional controller's output. (b) Individual cylinder trimming controls. (c) Switching-type EGO sensor located in tailpipe. (d) Linear-type EGO sensor in runner 2.

runner for cylinder 2; the latter sensor allows "direct" measurement[7] of the A/F, but its bandwidth is low.

For the test shown in Fig. 8, maldistribution was experimentally simulated by reducing the pulsewidth to cylinder 2 by 20%. Figs. 8(a) and 8(b) show that the conventional fuel controller was turned off and the individual cylinder fuel controller was turned on after about 75 engine events. The individual cylinder controller response shows the controller compensating for the 20% lean cylinder by increasing the pulsewidth correction factor for that cylinder to about 1.2. This effect is confirmed in Figs. 8(c) and 8(d) which show the reduction in the maldistribution (indicated by the switching EGO sensor) and the correction of the air-fuel ratio for cylinder 2 from 20% lean to stoichiometry (indicated by the linear EGO sensor). The engine in our test cell had some nominal maldistribution: 7% rich, 0%, 3.5% rich and 9% rich, on cylinders 1–4, respectively. The controller was able to bring the system to a balanced condition. The plots are quite similar to Fig. 8 and are not repeated here.

V. Conclusion

The fuel management system on a modern automobile must act in concert with the three-way catalytic converter (TWC) to achieve the low levels of HC, CO, and NOx emissions currently mandated. Typically, there is only a very narrow range of A/F near the stoichiometric value (14.64) over which high simultaneous conversion efficiencies may be attained, and this can be adversely affected by cylinder-to-cylinder maldistribution.

This paper has provided an approach to achieving uniform cylinder-to-cylinder air-fuel ratio control, in the face of injector mismatch and unbalanced airflow due to engine geometry, using only the existing switching-type EGO sensor common on today's automobiles. The controller design from modeling to successful experimental implementation in a dynamometer test facility was reported. The controller's design was based on a very simple model, the validity of which was extended by implementing a variable sampling schedule, rather than by employing traditional gain scheduling.

[7]Recall, the sensor actually measures the partial pressure of oxygen; moreover, the exhaust gases at this point are not full equilibrated.

Acknowledgment

The authors thank P. Roth for his assistance in experimentally validating the controller, M. T. Pallett for his help in programming the data acquisition system, J. Young for his work on simulating some of the initial controller designs, and M. Smokovitz for the custom electronics. G. Lawson is sincerely thanked for making the facilities available to us. The advice of D. Hamburg on A/F modeling and control was invaluable.

REFERENCES

[1] M. A. Shulman and D. R. Hamburg, "Non-ideal properties of Z_rO_2 and T_iO_2 exhaust gas oxygen sensors," SAE Tech. Paper Series, no. 800018, 1980.

[2] D. R. Hamburg, J. A. Cook, W. J. Kaiser and E. M. Logothetis, "An engine-dynamometer study of the A/F compatibility between a three-way catalyst and an exhaust gas oxygen sensor," SAE Tech. Paper Series, no. 830986, 1983.

[3] A. D. Colvin, J. W. Butler, and J. E. Anderson, "Catalytic effects on Z_rO_2 oxygen sensors exposed to non-equilibrium gas mixtures," *J. Electroanal. Chem.*, vol. 136, pp. 179–183, 1982.

[4] J. A. Cook, D. R. Hamburg, W. J. Kaiser and E. M. Logothetis, "Engine dynamometer study of the transient response of ZrO_2 and TiO_2 exhaust gas oxygen sensors," SAE Tech. Paper Series, no. 830985, 1983.

[5] P. P. Khargonekar, K. Poolla, and A. Tannenbaum, "Robust control of linear time-invariant plants using periodic compensation," *IEEE Trans. Automat. Contr.*, vol. AC-30, pp. 1088–1096, 1985.

[6] T. Haigawara and M. Araki, "Design of a stable state feedback controller based on the multirate sampling of the plant output," *IEEE Trans. Automat. Contr.*, vol. 33, pp. 812–819, 1988.

[7] B. A. Francis and T. T. Georgiou, "Stability theory of linear time-invariant plants with periodic digital controllers," *IEEE Trans. Automat. Contr.*, vol. 33, pp. 820–832, 1988.

[8] K. L. Buescher, "Representation, analysis, and design of multirate discrete-time control systems," M.S. thesis, Dept. of Elec. Comput. Eng., Univ. Illinois, Urbana-Champaign, 1988.

[9] M. C. Berg, N. Amit, and J. D. Powell, "Multirate digital control system design," *IEEE Trans. Automat. Contr.*, vol. 33, pp. 1139–1150, 1988.

[10] J. M. Maciejowski, "Asymptotic recovery for discrete-time systems," *IEEE Trans. Automat. Contr.*, vol. AC-30, pp. 602–605, 1985.

[11] J. A. Cook and B. K. Powell, "Discrete simplified external linearization and analytical comparison of IC engine families," in *Proc. Am. Contr. Conf.*, Minneapolis, MN, June 1987, pp. 325–333.

[12] B. K. Powell, G. P. Lawson, and G. Hogh, "Advanced real time powertrain systems analysis," *ASME Trans. J. Eng. for Gas Turbines and Power*, vol. 110, no. 3, pp. 325–333, July 1988.

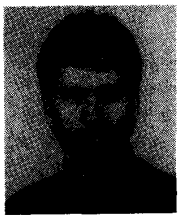

Jessy W. Grizzle (S'78–M'83–SM'90) was born on February 8, 1957. He received the B.S.E.E. degree from Oklahoma State University, Stillwater, in 1979, and the M.S.E. and Ph.D. degrees in electrical engineering from The University of Texas at Austin, in 1980 and 1983, respectively.

From January to December 1984, he was at the Laboratoire des Signaux et Systèmes, Gif-sur-Yvette, France. From January 1984 to August 1987, he was an Assistant Professor in the Department of Electrical Engineering, University of Illinois at Urbana-Champaign. Since September 1987, he has been with the Department of Electrical Engineering and Computer Science, The University of Michigan, Ann Arbor, where he is currently an Associate Professor. His major research interests include nonlinear system theory, geometric methods, and multirate digital systems.

Dr. Grizzle was a (full) Fulbright Grant awardee and a NATO Postdoctoral Fellow from January to December 1984. He received a Presidential Young Investigator Award in 1987. He is an Associate Editor of the IEEE TRANSACTIONS ON AUTOMATIC CONTROL and of *Systems and Control Letters*.

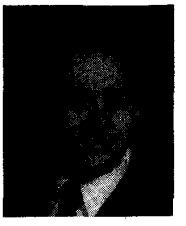

Kelvin L. Dobbins received the B.S.M.E. degree from Texas Tech University, Lubbock, in 1980, and the M.S.E. and Ph.D. degrees in mechanical engineering from The University of Texas, Austin, in 1982 and 1985, respectively.

He joined the Ford Motor Company, Dearborn, MI, in 1985 in the Control Systems Department of Research Staff where he is engaged in the area of vehicle emission control systems.

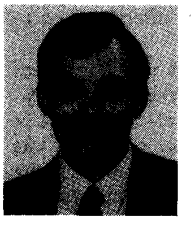

Jeffrey A. Cook (A'85) received the B.S. degree in mechanical engineering from The Ohio State University, Columbus, in 1973, and the M.S. degree in electronics and computer control from Wayne State University, Detroit, MI, in 1985.

He joined the Ford Motor Company, Dearborn, MI, in 1976, where he is a Research Engineer in the Control Systems Department. His research interest is air-fuel ratio and emissions control for internal combustion engines.